

Divergence control of multi-MeV laser accelerated proton beams using curved foil targets

K. Markey, S. Kar, P. Simpson, B. Dromey and M. Zepf

Centre for Plasma Physics, Queen's University Belfast, Belfast, BT7 1NN, UK

C. Bellei, S. Nagel, S. Kneip, Z. Najmudin and L. Willingale

Blackett Laboratory, Imperial College, London SW7 2BZ, UK

K. Krushelnick

University of Michigan, Ann Arbor, MI 48109, USA

J. S. Green, P. A. Norreys, R. J. Clarke and D. Neely

Central Laser Facility, STFC, Rutherford Appleton Laboratory, HSIC, Didcot, Oxon OX11 0QX, UK

D. C. Carroll and P. McKenna

Department of Physics, University of Strathclyde, Glasgow G4 0NG, UK

E. L. Clark

Technological Educational Institute of Crete, Branch of Chania, Romanou 3, Chalepa, Chania, Crete, Greece 73133

Contact | m.zepf@qub.ac.uk

Introduction

Ongoing advances in high power, short pulse laser technology have created many new, inter-related fields of research. An exciting prospect is the generation of multi-MeV ions with compact tabletop laser systems^[1-3] and the use of such high peak current beams in a variety of applications.

When a high intensity laser pulse is incident on a thin foil, the leading edge of the pulse rapidly ionizes the material creating a solid density plasma. Electrons in the laser focus are heated to temperatures of the order of the laser ponderomotive potential, typically several MeV. The hot electrons propagate through the target to the rear surface. Here the electron cloud is confined to the planar surface by the large electrostatic field induced by the charge separation. Field strengths of 10^{12} V/m are typically present in the electrostatic sheath and the rear surface ions are accelerated to MeV energies over tens of microns. This process is termed target normal sheath acceleration (TNSA)^[4].

Typically the surface layers experiencing the peak sheath field contain high concentrations of hydrogen regardless of the bulk target material. Protons are thus the most energetic particles accelerated by the charge separation field.

Typical proton beams are emitted normal to the target surface with energy dependent divergence – the peak energy protons have the lowest divergence and originate from a small region on the rear surface corresponding to the peak sheath field while the more numerous lower energy protons originate from a much larger area of the foil rear surface and are typically emitted into 40°- 60° cone angles. This divergence limits the useable flux of protons for several applications such as isochoric heating and injection into additional acceleration structures such as phase rotators^[5] or energy selection structures such as the laser triggered microlens^[6] etc.

The proton beams exhibit very good laminarity, with the most divergent protons originating from the outer extent of the proton source region. A simple approach to control the divergence, involves the use of curved foils to collimate or focus the proton beam^[7-9]. This was subsequently

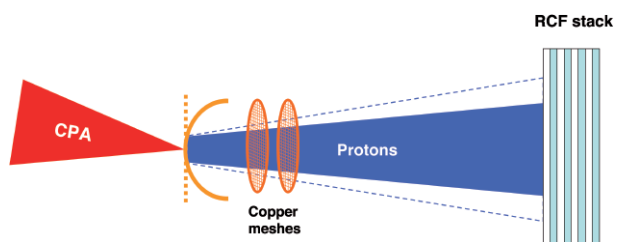


Figure 1. Experimental setup, showing the beam envelopes from the curved (solid) and planar (dashed) targets.

demonstrated for low proton energies (≤ 3.5 MeV) by Patel *et al.*^[8] and Snaveley *et al.*^[9].

Here we present results from an experiment to investigate the effect of foil curvature on proton beam divergence in the tens of MeV energy range.

Experiment

The experiment was carried out on the Vulcan Petawatt laser. The laser delivered ~ 350 J of energy to the target in a 600 fs FWHM pulse. Firstly, 15 μm thick gold foils, cylindrically curved with radii of curvature of 1 mm, 2 mm and 3 mm were irradiated with the laser focused to a 20 μm focal spot to give a laser intensity of 2×10^{20} W/cm². Secondly a 250 μm tin foil, cylindrically curved with a radius of curvature of 0.35 mm was irradiated with the laser focused to an intensity of 6×10^{20} W/cm². In each case, planar reference foils were also irradiated for comparison. The emitted protons were detected with stacks of radiochromic film (RCF), a dosimetry detector sensitive to proton energy deposition (figure 1). The proton dose recorded on each layer of RCF corresponded predominantly to a narrow spectral energy interval. Thus it was possible to characterize the beam profile at discrete intervals over the entire proton energy range.

To map the beam expansion in the vicinity of the foil two copper meshes were placed in the beam path. The thin mesh imprints were visible in the beam profile on the RCF

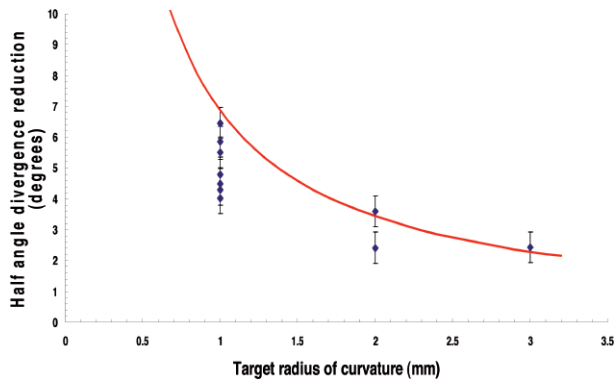


Figure 2. Half angle divergence reduction of 17.5 MeV proton beams plotted as a function of target radius of curvature. The solid line indicates the ballistic model prediction assuming a 120 μm proton source radius for all targets at this energy.

and enabled the size of the beam at the meshes to be determined. Additionally it was possible to calculate the virtual source position of the protons using the multiple beam size measurements along the beam path.

Results

In clear contrast to the highly circular beam profiles detected from planar foils, beam profiles from the curved 15 μm gold foils were seen be elliptical. The vertical dimension, corresponding to the planar dimension of the hemicylinder was seen to remain unchanged and similar to the flat foil case. The beam envelope size at the RCF in the horizontal dimension was reduced with a clear trend of larger reductions for decreasing radii of curvature (figure 2).

Although laser produced proton beams originate from sources of up to several hundred microns in diameter, the laminar accelerating field of the sheath is such that the resultant particle trajectories can be traced to a point-like virtual source. This virtual source can be determined using

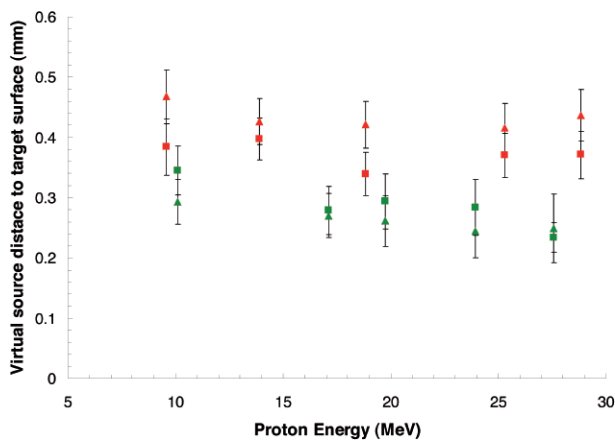


Figure 3. Virtual source positions (on the detector side of the target) versus proton energy for proton beams from a planar (red) and hemicylindrical target with a 1 mm radius of curvature (green). The virtual sources were measured in both the horizontal (squares) and vertical (triangles) plane for both targets.

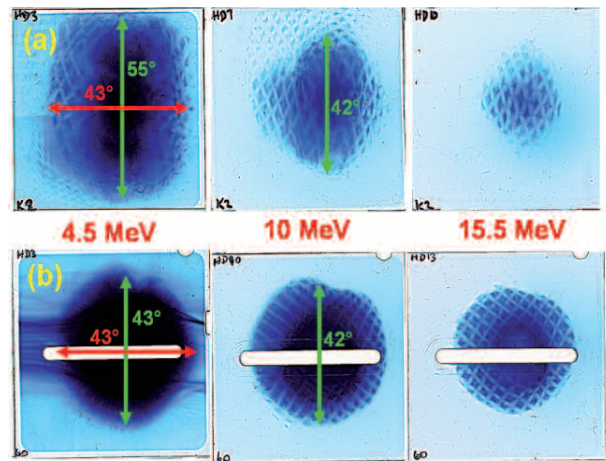


Figure 4. Example RCF layers for (a) the 250 μm tin hemicylinder with a 0.35 mm radius of curvature (the vertical dimension corresponds to the target curvature) and (b) the planar reference foil of identical material and thickness.

a linear fit between the measurements of the beam envelope sizes at the mesh and RCF planes^[10]. The virtual source position as a function of energy is plotted in figure 3 for the 15 μm planar reference foil and a typical hemicylinder with a radius of curvature of 1 mm.

The 250 μm tin foil was used as it is known that proton beams from thicker foils are less divergent. This property, coupled with the smaller target radius of curvature of 0.35 mm dramatically increases the effect on the beam envelope. Beam profiles are shown in figure 4 and indicate that the beam dimension is relatively unchanged in the vertical dimension (corresponding here to the uncurved dimension of the hemicylinder), compared to the flat reference case. The beam envelope size in the dimension of curvature is however increased at energies below 10 MeV. In this case only one mesh was visible. This mesh measurement enabled the proton beam virtual source to be measured as shown in figure 5.

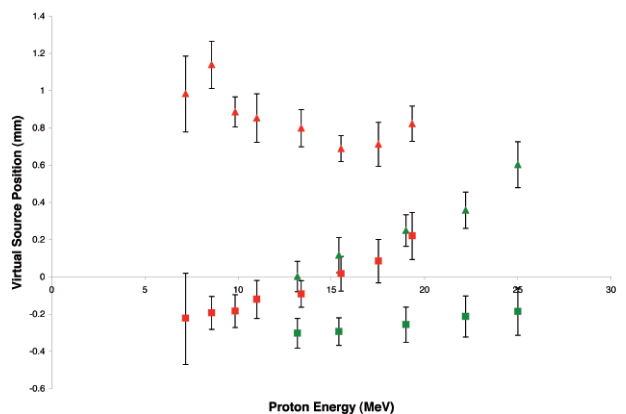


Figure 5. The virtual source position as measured in the horizontal (squares) and vertical (triangles) dimension for the 250 μm hemicylindrical (red) and planar (green) targets. The curved surface of the hemicylinder corresponds to the vertical dimension.

Discussion

A simple ballistic approximation of the curvature effect explains the scaling of the divergence reduction with radius of curvature. Assuming that protons travel in linear trajectories from the proton source region, the reduction in divergence from the flat foil case is the rotation of the target normal at the edge of the proton source region, i.e. $\Delta\theta = \theta_{\text{initial}} - \theta_{\text{final}} = r/R$ radians (see figure 6). For the proton energy of 17.5 MeV, a proton source radius of $\sim 120 \mu\text{m}$ is typical and gives good agreement between the ballistic model and the experimental data as shown in figure 2.

The virtual source position for the flat foil was located approximately $400 \mu\text{m}$ from the foil surface on the RCF side of the target. This result indicates that although the beam laminarity is evident by the clear mesh image on the RCF, the particle trajectories between the foil and the RCF stack are not linear. The double mesh measurements however indicate that the particle trajectories are linear between the two meshes and the RCF stack. This indicates that the beam envelope expands in a trumpet-like fashion for several hundred microns until it achieves its final divergence.

The virtual source positions of the curved foil proton beams were seen to deviate by $100 \mu\text{m}$ – $200 \mu\text{m}$ from the flat foil case but no clear dependence on radius of curvature was discernable. Notably there was no deviation between the virtual source position in the horizontal (curved) and vertical (planar) dimension. It is expected that the angular reductions achieved with the $15 \mu\text{m}$ gold foils may not affect the virtual source position dramatically. A shift of the virtual source position by $\sim 100 \mu\text{m}$ would be difficult to discern given the measurement uncertainty and shot to shot variation.

The curvature effect is much more extreme for the $250 \mu\text{m}$ thick target but still consistent with the ballistic approximation. Radial spreading of the electrons as they propagate through the target broadens the distribution at the rear surface. Electron energy losses inside the thicker target were partially compensated by the higher laser intensity employed with the tin targets so as to maintain significant proton numbers in the 10 MeV–20 MeV range. The broader electron distribution at the rear surface leads to less lateral spreading of the ions in the acceleration phase, explaining why the initial flat foil divergence is lower than for the $15 \mu\text{m}$ targets and the source size is estimated to be $\sim 500 \mu\text{m}$ for proton energies around 10 MeV. At this energy, from the ballistic model, $r/R = (250/350) = 0.7$ radians (41°). This implies the protons would focus at a point $\sim 1 \text{ mm}$ from the target rear surface and expand from the focus with a full cone angle of $\sim 40^\circ$. This is in excellent agreement with the measured virtual source position at this energy (figure 5) and the cone angle as inferred from the beam size at the RCF (figure 4). It was not possible to measure the virtual source position at low energies due to RCF saturation but the beam envelope exhibits clear evidence that as the source size increases, the focusing effect is more dramatic, resulting in a 55° cone angle at 4.5 MeV.

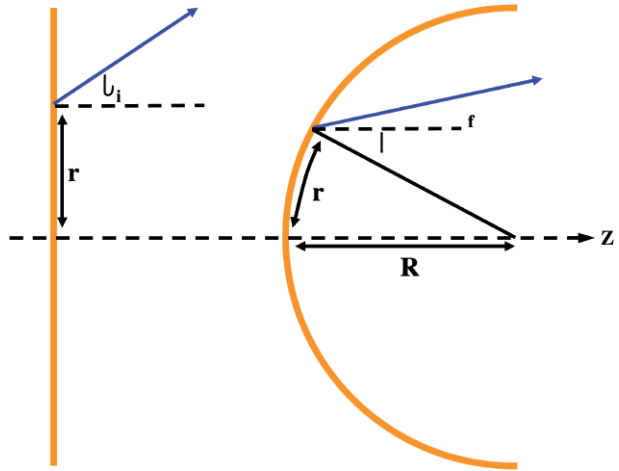


Figure 6. A simple ballistic model of the effect of target curvature on proton trajectories at the edge of the sheath region. $\Delta\theta$, the half angle reduction in beam divergence is simply φ , the angle subtended by the proton source radius at the foil centre of curvature, a distance R from the foil rear surface.

Conclusion

The use of curved foils to control proton beam divergence has been demonstrated at higher proton energies than previously reported. Reductions in the beam envelope divergence have been achieved in good agreement with a simple ballistic model.

Acknowledgements

The authors would like to acknowledge the assistance of the Vulcan and Target Fabrication staff of the Central Laser Facility at the Rutherford Appleton Laboratory.

References

1. S. Hatchett *et al.*, *Phys. Plasmas* **7**, 2076 (2000).
2. E. Clark *et al.*, *Phys. Rev. Lett.* **84**, 670 (2000).
3. R. A. Snavely *et al.*, *Phys. Rev. Lett.* **85**, 2945 (2000).
4. S. C. Wilks *et al.*, *Physics of Plasmas* **8**, 542 (2001).
5. A. Noda *et al.*, *Laser Physics* **16**, 647–653 (2006).
6. T. Toncian *et al.*, *Science* **312**, 410–413 (2006).
7. Y. Ueshima *et al.*, *Nuclear Instruments and Methods in Physics Research A* **455**, 181–184 (2000).
8. P. K. Patel *et al.*, *Phys. Rev. Lett.* **91**, 125004 (2003).
9. R. A. Snavely *et al.*, *Phys. Plasmas*, **14**, 092703 (2007).
10. M. Borghesi *et al.*, *Phys. Rev. Lett.* **92**, 055003 (2004).